

# Accuracy Analysis of Geometrical and Numerical Approaches for Two Degrees of Freedom Robot Manipulator

*By* Hendri Maja Saputra

# ACCURACY ANALYSIS OF GEOMETRICAL AND NUMERICAL APPROACHES FOR TWO DEGREES OF FREEDOM ROBOT MANIPULATOR

Hendri<sup>4</sup>aja Saputra<sup>a,\*</sup>, Midriem Mirdanies<sup>a</sup>, Estiko Rijanto<sup>a</sup>

<sup>a</sup>Research Center for Electrical Power and Mechatronics, Indonesian Institute of Sciences (LIPI),  
LIPI Office (PuslitTelimek, Building 20, 2<sup>nd</sup> floor), Jl. Cisit, No.21/154D, Bandung, 40135, Indonesia

Received 28 October 2016; received in revised form: 14 November 2016; accepted: 15 November 2016  
Published online: XX December 2016

## Abstract

Analysis of algorithms to determine the accuracy of aiming direction using two inverse kinematic approach i.e., geo-metric and numeric has been done. The best method needs to be specified to precisely and accurately control the aiming direction of a Two Degrees of Freedom (TDOF) manipulator. The manipulator degrees of freedom are azimuth (Az) and elevation (El) angles. A program has been made using C language to implement the algorithm. Analysis of the two algorithms was done using statistical approach and circular error probable (CEP). The research proves that accuracy percentage of numerical method is better than geometrical method, those are 98.63% and 98.55%, respectively. Based on the experiment results, the numerical approach is the right algorithm to be applied in the TDOF robot manipulator.

Keywords: azimuth; elevation; geometrical; numerical; C language.

## I. INTRODUCTION

Two degrees of freedom (TDOF) manipulator is a device that makes a modern instrument more convenient to be operated. Modern TDOF robot manipulator has been equipped with object detection and identify features using certain sensors, such as acoustic sensors and visual sensors. In the study conducted by Mirdanies [1], object detection and identification was performed using Kinect<sup>TM</sup> camera with sift and surf methods.

Visual sensors and algorithm are used to convert the coordinates of the target to the aiming direction which is the key in this technology. The algorithm will determine the accuracy and precision of the TDOF manipulator aiming direction. Formula of this algorithm is closely associated with the forward and inverse kinematic as in the science of robotics [2]. Inverse kinematic can be completed with two common approaches, i.e., geometrical and numerical [3] [4] approaches. Robotic or mechatronic systems that use high-speed

processing devices can use the numerical approach through iterative process of Jacobian matrix [6] for the inverse kinematic solution (Saputra & Rijanto, Analisis Kinematik dan Dinamik Mekanisme Penggerak 2-DOF untuk Antena Bergerak pada Komunikasi Satelit (Kinematic and dynamic analysis of a 2-DOF mechanism for mobile satellite communication) (SATCOM antennas), 2009) (Aristidou & Lasenby, Inverse Kinematics: A Review of Existing Techniques and Introduction of a New Fast Iterative Solver, 2009). Research on inverse kinematic via geometrical and numerical approach has been done by Feng [7] for PUMA 560, but the accuracy and precision issues are not discussed in detail. Especially for inverse kinematic via numerical approach, Tchou [8] has applied it to the stationary manipulators and mobile robots. In [12] numerical approach undertaken by Soeh [9], the extended Jacobian technique has been compared with the inverse Jacobian.

Kinect<sup>TM</sup> is used as visual sensor in this study. It is placed on a fixed base, so that coordinate transformation from a position at the manipulator

\* Corresponding Author. Tel: +6281381006059  
E-mail: hend018@lipi.go.id

is to be derived using the Denavit-Hartenberg (DH) notation [2].

This study aims to analyze the effect of using geometrical and numerical approaches to the accuracy and precision of a TDOF robot manipulator aiming direction.

## II. HOMOGENEOUS TRANSFORMATION MATRIX

Figure 1 illustrates coordinates system of the camera, the TDOF manipulator, and the pointed direction of a specific target. Homogeneous transformation matrix of the camera can be written in the form of ZYX Euler representation ( ${}^A_B R_{\alpha,\beta,\gamma}$ ) in combination with the translational vector [2]. Assuming that there is no change in orientation ( $\alpha = \beta = \gamma = 0$ ) and there is only translation along the X-axis ( $\Delta_x$ ), Y-axis ( $-\Delta_y$ ), and Z-axis ( $\Delta_z$ ) the camera homogeneous transformation  $T_c$  can be written as Eq. 1.

$$T_c = \begin{bmatrix} 1 & 0 & 0 & \Delta_x \\ 0 & 1 & 0 & -\Delta_y \\ 0 & 0 & 1 & \Delta_z \\ 0 & 0 & 0 & 1 \end{bmatrix} \quad (1)$$

Based on direct measurements in the mechanism it is known that  $\Delta_x$  value is 26.5 cm,  $\Delta_y$  is 1.25 cm, and  $\Delta_z$  is 0 cm.

The TDOF robot manipulator parameters in the DH notation [2] can be seen in Table 1. These parameters are used to calculate the coordinates of each point based on homogeneous transformations in Eq. 2. The calculation results of each link are shown by Eq. 3 and 4. Homogeneous transformation matrix of the manipulator from the tip relative to the base coordinates can be seen in Eq. 5.

Table 1.  
TDOF Robot Manipulator Parameters

Link - i	$\alpha_i$	$a_i$	$d_i$	$\theta_i$
1	$\pi/2$	0	$d_1$	$\theta_1$
2	0	$a_2$	0	$\theta_2$

$${}^{i-1}T_m = \begin{bmatrix} c \theta_i & -s \theta_i c \alpha_i & s \theta_i s \alpha_i & a_i c \theta_i \\ s \theta_i & c \theta_i c \alpha_i & -c \theta_i s \alpha_i & a_i s \theta_i \\ 0 & s \alpha_i & c \alpha_i & d_i \\ 0 & 0 & 0 & 1 \end{bmatrix} \quad (2)$$

$${}^0T_m = \begin{bmatrix} c \theta_1 & 0 & s \theta_1 & 0 \\ s \theta_1 & 0 & -c \theta_1 & 0 \\ 0 & 1 & 0 & d_1 \\ 0 & 0 & 0 & 1 \end{bmatrix} \quad (3)$$

$${}^1T_m = \begin{bmatrix} c \theta_2 & -s \theta_2 & 0 & a_2 c \theta_2 \\ s \theta_2 & c \theta_2 & 0 & a_2 s \theta_2 \\ 0 & 0 & 1 & 0 \\ 0 & 0 & 0 & 1 \end{bmatrix} \quad (4)$$

$${}^0T_m = \begin{bmatrix} c \theta_1 c \theta_2 & -c \theta_1 s \theta_2 & s \theta_1 & a_2 c \theta_1 c \theta_2 \\ s \theta_1 c \theta_2 & -s \theta_1 s \theta_2 & -c \theta_1 & a_2 s \theta_1 c \theta_2 \\ s \theta_2 & c \theta_2 & 0 & d_1 + a_2 s \theta_2 \\ 0 & 0 & 0 & 1 \end{bmatrix} \quad (5)$$

where  $s \theta_1 = \sin \theta_1$ ,  $c \theta_1 = \cos \theta_1$ ,  $s \theta_2 = \sin \theta_2$ , and  $c \theta_2 = \cos \theta_2$ .  $d_1$  represents length of link 1, and  $a_2$  is length of link 2. Based on measurements, it is known that  $d_1$  is 34.25 cm, whereas  $a_2$  is 40 cm.

The targets are assumed to be simply a translation along the X-axis ( $L_x$ ), thus homogeneous transformation matrix of the target referred to the tip of the link 2 can be written as Eq. 6.

$$T_T = \begin{bmatrix} 1 & 0 & 0 & L_x \\ 0 & 1 & 0 & 0 \\ 0 & 0 & 1 & 0 \\ 0 & 0 & 0 & 1 \end{bmatrix} \quad (6)$$

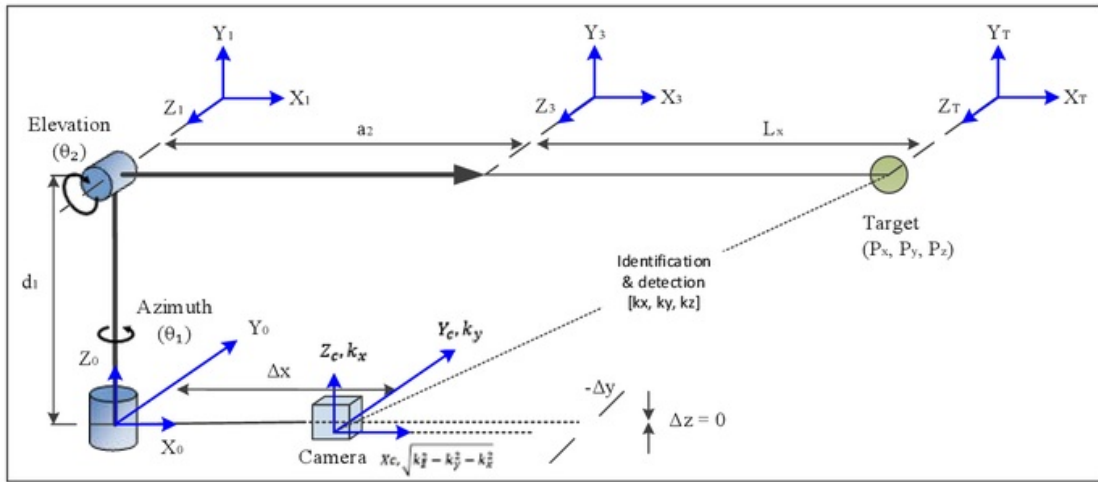


Figure 1. Coordinates system of camera, TDOF manipulator, and target point

The total homogeneous transformation matrix is obtained by multiplying homogeneous transformation matrices of the camera, the manipulator, and the target matrices as follows:

$$T = T_C * {}^0T_m * T_T = \begin{bmatrix} R & P \\ 0 & 1 \end{bmatrix} \quad (7)$$

where:

$$R = \begin{bmatrix} n_x & s_x & a_x \\ n_y & s_y & a_y \\ n_z & s_z & a_z \end{bmatrix} = \begin{bmatrix} c \theta_1 c \theta_2 & -c \theta_1 s \theta_2 & s \theta_1 \\ s \theta_1 c \theta_2 & -s \theta_1 s \theta_2 & -c \theta_1 \\ s \theta_2 & c \theta_2 & 0 \end{bmatrix} \quad (8)$$

$$P = \begin{bmatrix} (a_2 + L_x) & c \theta_1 c \theta_2 \\ (a_2 + L_x) & s \theta_1 c \theta_2 \\ d_1 + (a_2 + L_x) & s \theta_1 \end{bmatrix} + \begin{bmatrix} \Delta_x \\ -\Delta_y \\ \Delta_z \end{bmatrix}. \quad (9)$$

### III. INVERSE KINEMATICS

Coordinates system of the camera, as shown in Figure 11, the object being detected by the camera is expressed in the camera coordinate system as  $[k_x, k_y, k_z]$ . In the camera coordinate system, z-axis forms a straight line between the camera and the object, and  $k_z$  represents the distance between them in z-axis. Therefore, the coordinates of the object in the DH-coordinate system is given by the following equation:

$$P_d = \begin{bmatrix} P_x \\ P_y \\ P_z \end{bmatrix} = \begin{bmatrix} \sqrt{k_z^2 - k_y^2 - k_x^2} + \Delta_x \\ k_x - \Delta_y \\ k_y + \Delta_z \end{bmatrix} \quad (10)$$

#### A. Geometrical Approach

Figure 2 illustrates coordinates system which is used to derive inverse kinematics using geometrical approach. From trigonometric formula, the following equations are obtained [3]:

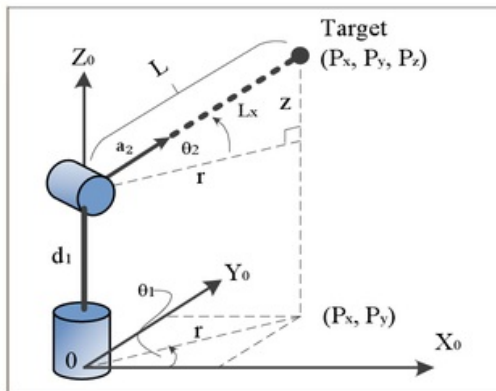


Figure 2. Geometrical approach coordinates

$$\left. \begin{aligned} \theta_1 &= \tan^{-1} \left( \frac{P_y}{P_x} \right) \\ \theta_2 &= \tan^{-1} \left( \frac{z}{r} \right) = \tan^{-1} \left( \frac{P_z - d_1}{\sqrt{P_x^2 + P_y^2}} \right) \end{aligned} \right\} \quad (11)$$

where  $\theta_1$  is rotation of joint on the horizontal plane which is called azimuth angle,  $\theta_2$  is rotation of joint on the vertical plane which is called elevation angle,  $(P_x, P_y, P_z)$  is the target coordinates relative to the manipulator base coordinate, and  $(d_1, a_2)$  is the length of the link 1 and link 2, respectively.

The distance  $L$  from the second joint to the target can be calculated as follows:

$$L = a_2 + L_x = \sqrt{P_x^2 + P_y^2 + (P_z - d_1)^2} \quad (12)$$

#### B. Numerical Approach

The algorithm of numerical approach is carried out through iteration process using pseudo-inverse Jacobian matrix [1] as Figure 3.

### IV. ACCURACY MEASUREMENT

In general, imprecise measurement is associated with random errors while inaccurate measurement is associated with systematic errors. Good aiming results will have small systematic and random errors, and vice versa. Systematic errors values are expressed by the difference between the average results of the aim with the midpoint of the target value, while random errors value is determined by the value of the standard deviation from the results of the aim [10].

Data can be analyzed under the assumption Gaussian (normal) distribution and independent of each other [11]. Gaussian is a distribution of data whose characteristics matches a probability density function (PDF) with average (mean)  $\mu$  and variance  $\sigma^2$ . Experiment results are data sets of points in horizontal axis (x) and vertical axis (y) in a window area generated by a laser pointer.

Once the impact point distribution has been assumed to be normal and independent in both dimensions, the dispersion of aiming points can be described using the circular error probable (CEP) [12, 13, 14, 15]. The CEP is often used to measure the level of accuracy in many applications [12]. CEP is defined as the radius  $r$  of a circle, centered about the target, which includes 50% of the aiming points [13, 15]. Estimation of CEP are based on means and standard deviations [13]. The use of CEP must meet four criteria: independence, normality, circular distribution, and mean point of impact (MPI) at the target. These criteria can be determined based on the general statistical tests.



Independence and MPI use the Student-test, normality using the Lillifors test, and circular distribution using the F-Test. In the aim results that have sampled the standard deviation of the

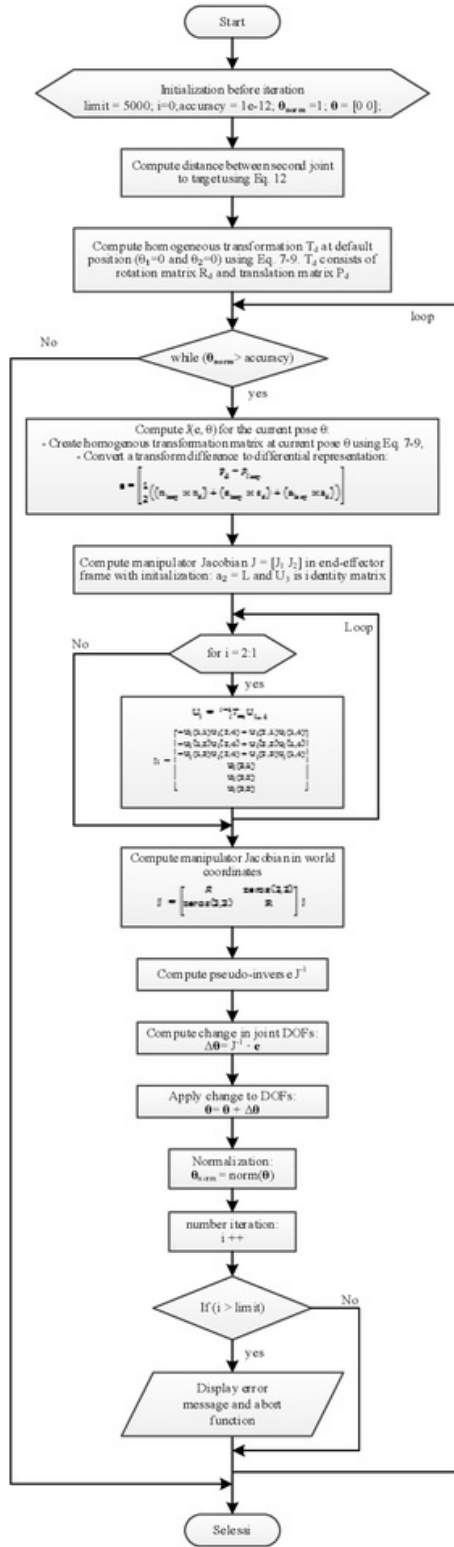


Figure 3. Geometrical approach coordinates

two coordinate axes, the CEP is calculated using Eq. 13. [12].

$$CEP = \begin{cases} (0.820k - 0.007)\sigma_s + 0.675\sigma_l & k < 0.3 \\ 0.615\sigma_s + 0.564\sigma_l & k \geq 0.3 \\ 1.177\sigma & k = 1 \end{cases} \quad (13)$$

where  $k$  is  $\sigma_s/\sigma_l$ ,  $\sigma_s$  is the smaller standard deviation,  $\sigma_l$  is the larger standard deviation, and  $\sigma$  is  $\sigma_x$  or  $\sigma_y$ .

In this paper, accuracy  $e$  is expressed in the form of percentage of accuracy level according to Eq.14.

$$e \% = \left(1 - \frac{\beta}{A}\right) \times 100\% \quad (14)$$

where  $\beta$  is radius of systematic error ( $\beta = \sqrt{\bar{x} + \bar{y}}$ ) and  $A$  is maximum radius of aiming area.

## V. EXPERIMENTAL SET-UP

The experimental set up is illustrated in Figure 4 and its working principle is shown in Figure 5. The target trajectory is represented by a linear and sinusoidal line input to produce movement of azimuth and elevation angles. It is given by the following equations.

$$\begin{cases} X_i = X_{i-1} + 20, \text{ for } 20 \leq X_i \leq 640 \\ Y_i = A_y \sin(2\pi f X_i + \phi_y) + b \end{cases} \quad (15)$$

where  $X_i$  and  $X_{i-1}$  are horizontal pixel along X-axis,  $Y_i$  is vertical pixel along Y-axis,  $A_y$  is sinusoidal gain,  $f$  is frequency, and  $b$  is offset.

The trajectory pixel data input is converted by the camera into trajectory coordinates  $(x,y)$ . The azimuth and elevation angles of the TDOF manipulator are computed using inverse kinematic and then the robot is driven by the motors so that the heading direction of the tip pin

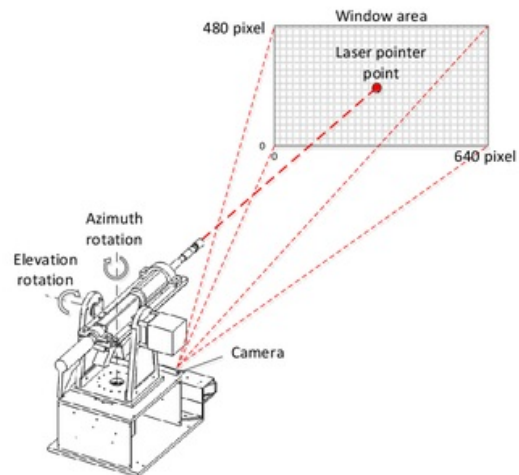


Figure 4. Experimental set-up. The heading direction is represented by a laser pointer on the window area (640x480 pixel) to be captured by the camera

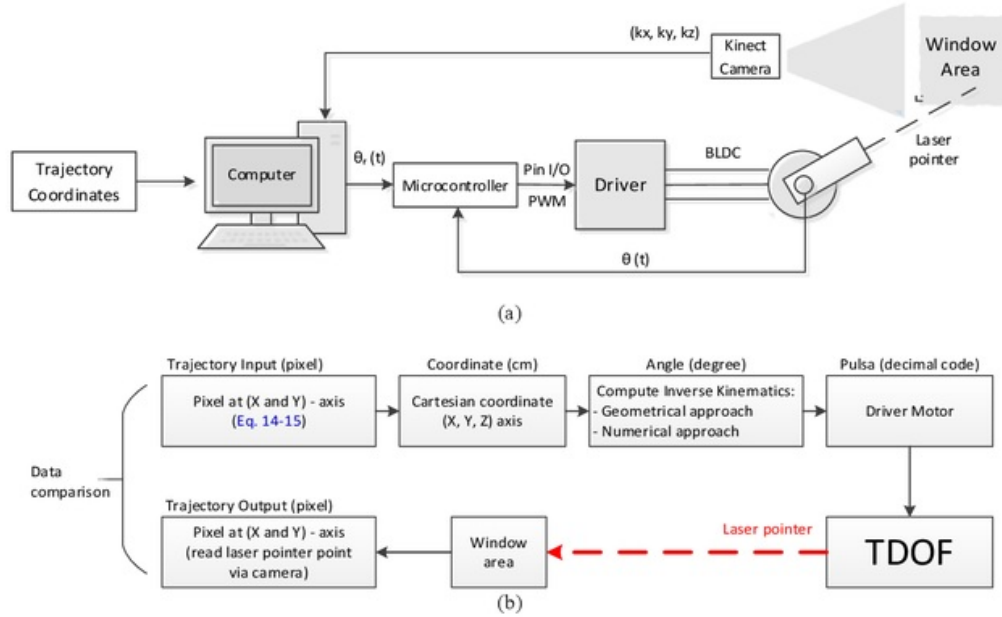


Figure 5. The working principle of experiment: (a) hardware set-up; (b) information flow

points to the trajectory coordinates by laser pointer.

The laser point (object) coordinates  $(x,y)$  and its distance is read by the camera. The trajectory pixel data output is compared with the trajectory pixel data input, Figure 6 plots the trajectory data input  $(kx, ky, kz)$ .

In practice, the microcontroller receives decimal values corresponding to the reference angle values from the host computer. In the experimental set up the following unit conversion holds: 1 pixel = 0.00176 cm = 0.00172 rad = 0.0984 deg. The resolution of input-output signal is 10 bits. From calibration through direct measurement, the relationship between angle and decimal value is given as follows:

$$D_{az} = -0.0002\theta_1^3 + -0.0001\theta_1^2 + 1.1492\theta_1 + 524.36 \quad (16)$$

$$D_{el} = -0.0004\theta_2^2 + 3.9254\theta_2 + 530.08 \quad (17)$$

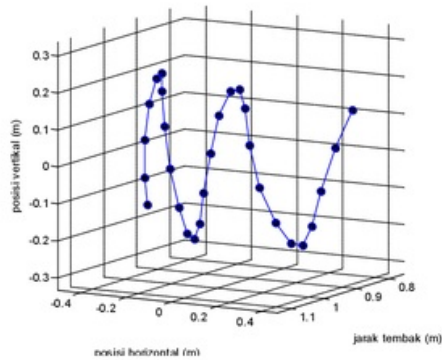


Figure 6. Isometric view of trajectory input

where  $D_{az}$  is a decimal value to enable azimuth rotation pulse, and  $D_{el}$  is a decimal value to enable elevation rotation pulse. The default position  $(0,0)$  of the TDOF manipulator in decimal is 526 (azimuth) and 530 (elevation).

## VI. RESULT AND ANALYSIS

A computer code has been made using C language to implement the algorithm. Figure 7 shows experiment results of aiming direction with 28 pieces of target coordinates. The solid black line is the reference target coordinates generated by equation (18), red broken line is output coordinates using geometrical approach, and the blue solid line is the output coordinate using numerical approach.

Performance indicators of error signal, i.e. average value ( $\mu$ ) and standard deviation ( $\sigma$ ), are

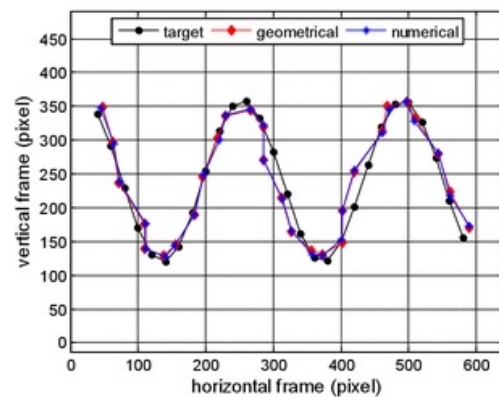


Figure 7. Experiment results

listed in Table 2. Processing time consumed by the host computer during the experiment was also recorded, and shown in Figure 8.

The maximum processing time required to calculate the inverse kinematic is 0.7  $\mu$ s for geometrical approach and 139.0  $\mu$ s for numerical approach. Average processing times of geometrical and numerical approaches are 0.4  $\mu$ s and 108.4  $\mu$ s, respectively. It can be said that the processing time of the numerical approach is 250 times longer than the geometrical approach.

The experiment result has been further analyzed in the form of aiming error as shown in Figure 9.

From Figure 9, it can be seen that the results of the aiming fall into the scope of the field tested, in other words, it has high accuracy and precision. By substituting performance indicator values in Table 2 into equation (17), relative accuracy percentage is obtained which is 98.55% for geometrical approach and 98.63% for numerical approach.

The experiment results were also analyzed statistically. Table 3 shows the details of statistical tests and values from CEP test data. It gives confidence level of 90% ( $\alpha = 0.1$ ). The statistical tests show generally good results. Special to the MPI test at the target, the population distribution at X axis produces critical  $t < t$  statistical which means it rejects null hypothesis. However, since  $p\text{-value} > 0.1$  (90%), this does not provide evidence to reject the null hypothesis that the MPI is not at the targets.

Table 2. Performance indicators of error signal

Parameter	geometrical		Numerical	
	X	Y	X	Y
mean, $\mu$	3.50	-0.11	3.32	0.29
deviation standard, $\sigma$	8.28	9.17	8.09	8.54
count, n	28.00	28.00	28.00	28.00
degree of freedom, $d_f$	27.00	27.00	27.00	27.00
$k = \sigma_{\min} / \sigma_{\max}$	0.90		0.95	

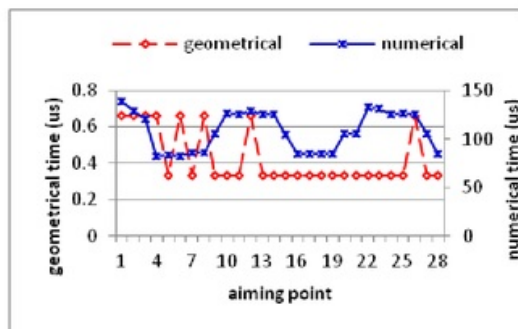


Figure 8. Processing time during experiment

The CEP plots can be seen in Figure 10. It appears that the CEP (50% probable) for the numerical approach is smaller than the geometrical approach, i.e. 10.27 pixels and 9.79 pixels, respectively.

## VII. CONCLUSION

The research proves that numerical method provides relative accuracy percentage which is better than geometric method, which is equal to 98.63% and 98.55%, respectively. Therefore, it can be recommended to implement the numerical algorithm into TDOF robot manipulator instead of the geometrical one.

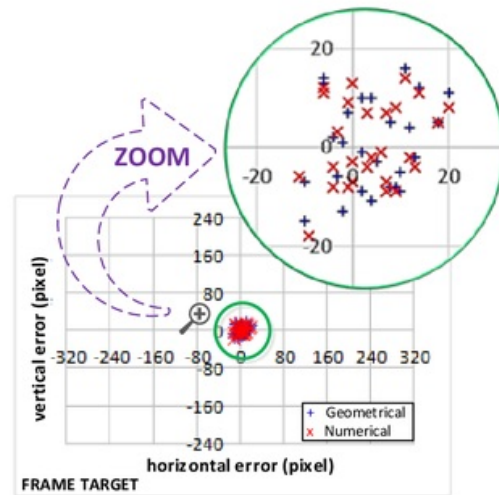


Figure 9. Processing time during experiment

Table 3. CEP statistical test details

CEP Results at ( $\alpha = 0,01$ )	Geometrical (pixel)		Numerical (pixel)	
	Az	El	Az	El
<b>t-Test for statistical independence</b>				
$\sigma^2$	68.63	84.10	65.41	72.88
$S^2_{pooled}$	76.36		69.14	
$d_f$	54.00		54.00	
t statistical	1.54		1.37	
t critical	1.67		1.67	
Independent:	YES		YES	
<b>Lilliefors Test for normality</b>				
t statistical	0.10	0.13	0.1	0.14
t critical	0.15		0.15	
Bivariate normal:	YES		YES	
<b>t-Test for MPI at target</b>				
t statistical	2.24	0.06	2.17	0.18
t critical	0.15		0.15	
MPI at the target:	NO	YES	NO	YES
p-value	0.98	0.52	0.98	0.57
<b>F-Test for circular distribution</b>				
F statistical	0.60		0.78	
F critical	1.65		1.65	
Circular:	YES		YES	
<b>CEP Results</b>				
CEP (about MPI)	10,27		9,79	



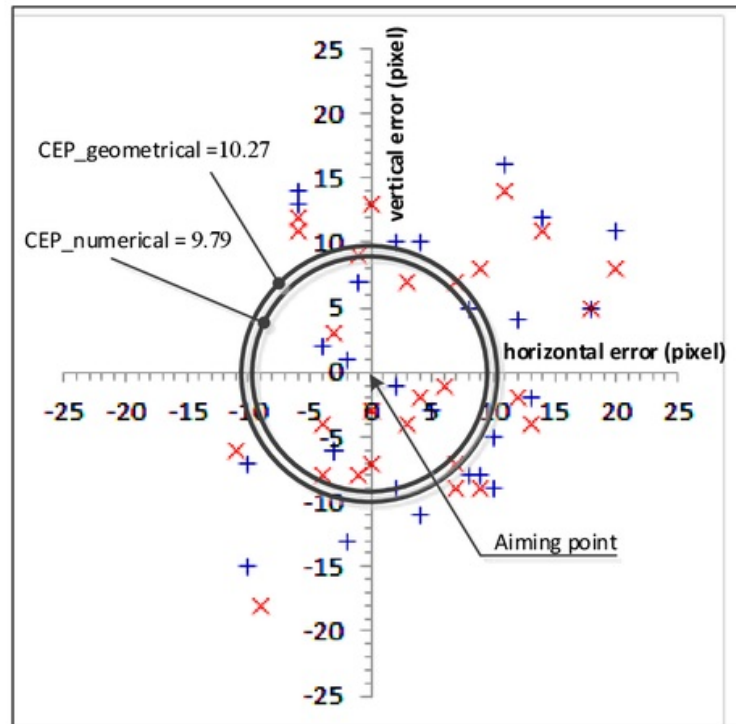


Figure 10. CEP result

## ACKNOWLEDGEMENT

This work was supported by the Research Center for Electrical Power and Mechatronics - LIPI, Indonesia. The authors would like to thank Aditya Sukma Nugraha M.T. who helped in the manufacture of the TDOF mechanism. Thanks also to Dr. Maria Margaretha Suliyanti who guided scientific paper writing.

## REFERENCES

- [1] M. Mirdanies, A. S. Prihatmanto dan E. Rijanto, "Object Recognition System in Remote Controlled Weapon Station using SIFT and SURF Methods," *Mechatronics, Electrical Power, and Vehicular Technology*, vol. 4, no. 2, pp. 99-108, 2013.
- [2] J. J. Craig, *Introduction to Robotics: Mechanics and Control*, Third penyunt., Canada: Pearson Prentice Hall, 2005.
- [3] H. M. Saputra, Z. Abidin dan E. Rijanto, "Analysis of Inverse Angle Method for Controlling Two Degree of Freedom Manipulator," *Mechatronics, Electrical Power, and Vehicular Technology*, vol. 3, no. 1, pp. 9-16, 2012.
- [4] H. M. Saputra, "Simulation of 2-DOF Mechanism Control System for Satellite Communication Antennas," Bandung, 2012.
- [5] H. M. Saputra dan E. Rijanto, "Analisis Kinematik dan Dinamik Mekanisme Penggerak 2-DOF untuk Antena Bergerak pada Komunikasi Satelit (Kinematic and dynamic analysis of a 2-DOF mechanism for mobile satellite communication (SATCOM) antennas)," *Teknologi Indonesia*, vol. 32, pp. 21-29, 2009.
- [6] A. Aristidou dan J. Lasenby, "Inverse Kinematics: A Review of Existing Techniques and Introduction of a New Fast Iterative Solver," 2009.
- [7] Y. Feng, W. Yao-Nan dan W. Shu-Ning, "Inverse Kinematic Solution for Robot Manipulator Based on Electromagnetism-like and Modified DFP Algorithms," *Acta Automatica Sinica*, vol. 37, no. 1, pp. 74-82, 2011.
- [8] K. Tchou, J. Karpinska dan M. Janiak, "Approximation of Jacobian Inverse Kinematics Algorithms," *Int. J. Appl. Math. Comput. Sci*, vol. 19, no. 4, pp. 519-531, 2009.
- [9] M. Soch dan R. Lorenez, "Solving Inverse Kinematics – A New Approach to the Extended Jacobian Technique," *Acta Polytechnica*, vol. 45, no. 2, pp. 21-26, 2005.
- [10] R. Taufiq, *Perancangan penelitian dan analisis data statistika*, Bandung: Penerbit ITB, 2006.
- [11] M. C. Anderson, "Generalize Weapon Effectiveness Modeling," Naval



- Postgraduate School, Monterey, California, 2004.
- [12] R. T. Jorris dan B. M. Young, "Design of Experiments and Analysis Examples from USAF Test Pilot School," dalam *U.S. Air Force T&E Days 2010*, Nashville, Tennessee, 2010.
- [13] C. McMillan dan P. McMillan, "Characterizing rifle performance using circular error probable measured via a flatbed scanner," dalam *Version 1.01 ed: Creative Commons Attribution-Noncommercial-No Derivative Works 3.0 United States License*, 2008.
- [14] Y. Wang, G. Yang, D. Yan, Y. Wang dan X. Song, "Comprehensive Assessment Algorithm for Calculating CEP of Positioning Accuracy," *Measurement*, vol. 47, pp. 255-263, 2014.
- [15] A. Didonato, "Computation of the Circular Error Probable (CEP) and Confidence Intervals in Bombing Test," Dahlgren Division Naval Surface Warfare Center NSWCDD/TR-07/13, Dahlgren, Virginia, 2007.

# Accuracy Analysis of Geometrical and Numerical Approaches for Two Degrees of Freedom Robot Manipulator

ORIGINALITY REPORT

6%

SIMILARITY INDEX

## PRIMARY SOURCES

- 1 Jorris, Timothy, Michael Young, and Elwood Waddell, Jr.. "Design of Experiments and Analysis examples from USAF Test Pilot School", U S Air Force T& E Days 2010, 2010. 34 words — 1%

Crossref
- 2 Saputra, Hendri Maja, Arif Santoso, Midriem Mirdanies, Vikita Windarwati, Riastus Nayanti, and Lukni Maulana. "Control of Pan-tilt Mechanism Angle using Position Matrix Method", Mechatronics Electrical Power and Vehicular Technology, 2013. 21 words — 1%

Crossref
- 3 Saputra, Hendri Maja, Zainal Abidin, and Estiko Rijanto. "IMU Application in Measurement of Vehicle Position and Orientation for Controlling a Pan-Tilt Mechanism", Mechatronics Electrical Power and Vehicular Technology, 2013. 20 words — 1%

Crossref
- 4 Saputra, Hendri Maja, and Midriem Mirdanies. "Controlling Unmanned Ground Vehicle Via 4 Channel Remote Control", Energy Procedia, 2015. 20 words — 1%

Crossref
- 5 Samadani, Ali-Akbar, Dana Kulic, and Rob Gorbet. "Multi-constrained inverse kinematics for the human hand", 2012 Annual International Conference of the IEEE Engineering in Medicine and Biology Society, 2012. 17 words — 1%

Crossref
- 6 [www.telimek.lipi.go.id](http://www.telimek.lipi.go.id) 15 words — < 1%

Internet
- 7 K HASHIMOTO. "Observer-Based Visual Servoing", Control in

---

Robotics and Automation, 1999

Crossref

14 words — < 1%

---

8 [jti.lipi.go.id](http://jti.lipi.go.id)

Internet

10 words — < 1%

---

9 [www.statshooting.com](http://www.statshooting.com)

Internet

9 words — < 1%

---

10 [Lecture Notes in Computer Science, 2016.](#)

Crossref

8 words — < 1%

---

11 H. Kimura. "Manipulator control with image-based  
visual servo", Proceedings 1991 IEEE

International Conference on Robotics and Automation, 1991

Crossref

8 words — < 1%

---

12 [ctn.cvut.cz](http://ctn.cvut.cz)

Internet

8 words — < 1%

---

13 Rijanto, Estiko, Hendri Maja Saputra, and  
Midriem Mirdanies. "Recent results of robotics R  
& D in the Indonesian Institute of Sciences: Mobile robot,  
articulated robot, pan tilt mechanism, and object recognition",  
2015 International Conference on Advanced Mechatronics  
Intelligent Manufacture and Industrial Automation (ICAMIMIA),  
2015.

Crossref

8 words — < 1%

---

EXCLUDE QUOTES OFF

EXCLUDE MATCHES OFF

EXCLUDE BIBLIOGRAPHY ON